Optimization of Engineering and Solvent Resistive Behavior of High Vinyl Acetate Content EVA-Modified Poly(ethylene-*co*-1-octene) Interpenetrating Network Blends Using Taguchi Orthogonal Array

Rumiya Pervin,[1] Luna Goswami,[2] V. Vijayabaskar,[3] Abhijit Bandyopadhyay[1]

[1]*Department of Polymer Science and Technology, University of Calcutta, Kolkata 700009, West Bengal, India*
[2]*KIIT School of Biotechnology, KIIT University Campus-XI, Patia Bhubaneswar 751024, Orissa, India*
[3]*Product Development Centre, Balmer Lawrie and Company Limited, Manali, Chennai, India*

Received 15 March 2011; accepted 19 December 2011
DOI 10.1002/app.36684
Published online in Wiley Online Library (wileyonlinelibrary.com).

ABSTRACT: Process parameters of poly (ethylene-*co*-vinyl acetate) (EVA)-modified poly (ethylene-*co*-1-octene) (POE)-interpenetrating, double network blend was designed through Taguchi L9 orthogonal array as a novel approach for complete optimization of engineering and solvent-swelling properties. Influence of different factors like EVA and peroxide concentrations, blending temperature, and blending time on gel content, tensile modulus, tensile strength, ultimate elongation were statistically calculated. Results showed good correlation between mathematical and physical inferences. Stress relaxation, hysteresis and other physico-mechanicals like total elongation, solvent-swelling, etc., were interestingly depended upon the nature of dominantly crosslinked phase instead of net crosslinking of the network hybrids. Sorption, on the other hand, depended on the hydrophobic-hydrophilic property of the surfaces. The series of data produced finally helped to select the best process parameters under which a particular POE-EVA blend composition yielded most balanced physico-mechanicals. © 2012 Wiley Periodicals, Inc. J Appl Polym Sci 000: 000–000, 2012

Key words: poly(ethylene-*co*-1octene); elastomer; interpenetrating; blends; mechanical properties; relaxation

INTRODUCTION

Metallocene-based poly (ethylene-*co*-1-octene) elastomer (POE) has received much attention recently due to several advantages like uniform comonomer content and controlled level of long chain branching, narrow molecular weight distribution, improved flexibility, and impact performance.[1,2] It also has excellent heat and UV stability. However, it is not been a popular choice industrially due to its poor processibilty. Also, its completely hydrophobic microstructure offers instability (poor solvent resistance) towards various industrial oils. Techniques such as conventional blending with polymers of similar microstructure, e.g., low density polyethylene (LDPE),[3] polypropylene (PP)[4–6], etc., graft copolymerizations with monomers like acrylic acid[7,8] silanes,[9] etc., are recently reported for property modification of POE. Use of pretreated fillers like electron beam irradiated clay[10] and nanodiamonds[11] in POE are also reported.

Reactive blending has been a novel and effective route to polymer modification known since number of years.[12–14] Interpenetrating networking (IPN), as a part of this unique blending process, is often adopted for confining two dissimilar polymers together. It is frequently practiced in solution phase but instances of such networking in molten state are rare. We, in our previous project, had successfully explored this with POE using high MFI (melt flow index, defined as the grams of polymer coming out of a standard aperture at 190°C within 10 min after 1 min preheating under a load of 2.16 kg) grade ethylene-*co*-acrylic acid (EAA) as modifier and dicumyl peroxide (DCP) as crosslinker.[15] Ethylene-*co*-vinyl acetate (EVA) with 40% vinyl ace-*co*-tate has been selected as the modifier in this project. There are no previous investigations reported on POE-EVA reactive blending other than the article by Horng-Jer Tai in 2001, who had reported random crosslinking between POE and EVA in presence of polyfunctional monomer triallyl cyanurate (TAC).[16] The study involved Monte Carlo simulation and gel content measurement for structure analysis of randomly

Correspondence to: A. Bandyopadhyay (abpoly@caluniv.ac.in).

Contract grant sponsor: Department of Science and Technology, Government of India; contract grant number: SR/FTP/ETA-23/08.

crosslinked low vinyl acetate containing EVA and POE. EVA with 40% vinyl acetate is extremely rubbery and has different flow property (high MFI) than the low vinyl acetate grade previously explored. Additionally, TAC is susceptible towards moisture hydrolysis and this could offer inconsistency in blend morphology. A solid acrylate-based compound of patented composition instead of TAC, devoid of this limitation, has been used as novel coagent for DCP in this project.

Taguchi statistical design of experiment (DOE) tool has been explored in this project as a novel way of optimizing engineering properties of POE-EVA reactive blends. Four primary factors were selected for the design: EVA content, DCP concentration, reaction/blending temperature and reaction time and each of these factors was varied for three different levels for complete optimization. The range of values set for each factors were selected from literature. The statistical tool has reduced total number of experiments from 81 (3^4) to only 9 by selecting L9 orthogonal array.[17] Our intention is to select a particular set of design parameters and a blend composition which offers an extraordinary combination of high tensile strength, moduli, and elongation properties but low hysteresis loss and faster stress relaxation, high surface polarity, and solvent resistance. Taguchi technique was preferred over other factorial designs since it is a unique tool which handles heterogeneous designs such as the present one (disparity between number of variables and their levels, i.e., four variables at three levels). Effect of coagent concentration was not considered as parameter during experiment design since it was found ineffective in altering mechanical properties.

TABLE I
Sample Composition and Experiment Details as per Taguchi L9 DOE

Samples	Experiment number	EVA content (wt %)[a]	Peroxide content (wt %)[b]	Temperature (°C)	Time (min)
S1	1	12.6 (1)	0.5 (1)	180 (1)	2 (1)
S2	2	25.1 (2)	0.5 (1)	220 (3)	4 (2)
S3	3	50.0 (3)	0.5 (1)	200 (2)	6 (3)
S4	4	12.6 (1)	1.0 (2)	200 (2)	4 (2)
S5	5	25.1 (2)	1.0 (2)	180 (1)	6 (3)
S6	6	50.0 (3)	1.0 (2)	220 (3)	2 (1)
S7	7	12.6 (1)	2.0 (3)	220 (3)	6 (3)
S8	8	25.1 (2)	2.0 (3)	200 (2)	2 (1)
S9	9	50.0 (3)	2.0 (3)	180 (1)	4 (2)

The figures in the parentheses indicate three different levels of each design parameters.

[a] The EVA concentration was with respect to 100 parts POE.

[b] Peroxide concentrations are applicable to individual POE and EVA to achieve double network structure.

EXPERIMENTAL

Materials

Poly (ethylene-*co*-1-octene) (POE) of MFI 5.0, % total crystallinity 19 and density 870 kg/m^3 was procured from Dow Chemicals (Switzerland). Poly (ethylene-*co*-vinyl acetate) of 40% vinyl acetate content with MFI 3.0 and density 967 kg/m^3 was generously supplied by Nicco Cables (Shyamnagar, India). Dicumyl peroxide (DCP, 98% purity) was procured from Aldrich Chemicals and was used without any further treatment. Coagent, an acrylate-based organic compound with patented composition, AUROSIN-6860, was kindly donated by Auropol India (India).

Preparation of interpenetrating network blends

Brabender Plastograph^R made in Germany TYP 815606 was used for reactive melt blending of the polymers at different process conditions. EVA was premixed with DCP and coagents (fixed at 1% with respect to DCP added) at 120°C for 1 min after 1 min preheating allowance (Stage I mixing). Similarly, POE was preblended with DCP and coagent at 120°C for 1 min after same preheating allowance (Stage I mixing). Finally, the temperature of the chamber was raised to the proposed blending temperature (Table I). Preblended POE was preheated at those temperatures for another 1 min and was finally blended with premixed EVA for stipulated time interval as proposed in Table I (Stage II mixing). Final batch weight was 40 g blended with a fill factor of 70%. Blends were taken out, palletized, and compression molded in a hydraulic press (S. C. Dey, Kolkata, India) at 180°C under 15 ton pressure for 5 min. The pressure was released after room temperature was attained.

Evaluation of physico-mechanical properties

Determination of gel content by solvent extraction method

Gel content of all the blends were measured after extracting with hot toluene (toluene was the common solvent) in a soxhlet apparatus for 24 h. The undissolved portion of the samples was assigned as gel. Gels were air-dried to constant weight to remove the associated solvents and the final weight was taken to calculate (eq. 1) the gel percentage for each composition:

$$\%\,\text{Gel} = (\text{Weight of the remnant sample})/(\text{Initial weight of the sample}) \times 100 \quad (1)$$

Studies on relative measure of crosslinking and chain scission

The remaining amount, i.e., (100% Gel Content) gives the percentage of sol content, i.e., the portion

of polymer dissolved in solvent. Using the sol content data of each blend a comparative study of chain scission and crosslinking was done with the help of Charlesby-Pinner plot made from the following equation (eq. 2)

$$S + S^{1/2} = \mu/\gamma + 1/(\gamma P_{N,0}[I_0]) \quad (2)$$

S denotes sol fraction, μ and γ are the probabilities of chain scission and crosslinking, $P_{N,0}$ is the number average chain length of the original polymer and (I_0) is the initial peroxide concentration. These parameters can be calculated from $S + S^{1/2}$ versus (I_0) plot for series of samples.

Fourier transform infrared spectroscopic analysis

Fourier transform infrared (FTIR) spectroscopic analysis of the gels was carried out to understand relative distribution of different polymers that was crosslinked. The study was done using a JASCO FTIR spectrophotometer within the spectral range of 400 to 4000 cm^{-1} in dispersive mode with a resolution of 4 cm^{-1}. An average of 120 scans for each sample was reported for analysis.

Transmission electron microscopic analysis

Transmission electron microscopic (TEM) analysis (model C-12, Philips) of selected network hybrids was carried out on thin films of average thickness 110 nm. The films were cut at $-90^{\circ}C$ in liquid nitrogen atmosphere in an automated cryocutter and were placed on copper grids of 300 mesh size. The samples were analyzed under an acceleration voltage of 120 kV.

Studies on mechanical properties

A steel die constructed in accordance to ASTM D412 was used to punch out dumbbell-shaped specimens from the blended sheets. All the mechanical properties were studied in a Universal Testing Machine (UTM LLOYD instrument LR 10 K plus, Load Cell 10 KN) at room temperature.

Tensile properties

Tensile properties including ultimate tensile strength, tensile modulus (@300%), and ultimate elongation was studied using a strain rate of 500 mm/min. All the measurements were carried out at room temperature until specimens ruptured. Ten specimens for each blend composition was tested and reported for analysis.

Stress relaxation test

Stress relaxation test was performed by quickly pulling the sample (strain rate was 500 mm/min) up to 100% elongation and then holding it until the decaying stress attained a constant value. The elongation was kept constant at the specified value and residual stress was measured with time. Each specimen was tested for 10 times and the average result has been reported for accuracy of the measurement. Using stress relaxation data relaxation time (λ) was calculated using eqs. (3) and (4) stated below

$$S = S_0 e^{(-t/\lambda)} \quad (3)$$

$$\ln S = \ln S_0 - t/\lambda \quad (4)$$

(S = stress at different time t and S_0 = stress at zero time i.e., initial stress).

λ was calculated from slope of the plot ln S vs. t (eq. 4).

Hysteresis measurement

Hysteresis test was performed straining the specimens up to 100% elongation at 50 mm/min cross head speed for three consecutive cycles at room temperature. Stress and elongation values were noted down for loading and unloading cycles and the corresponding loops were constructed.

Studies on solvent resistance behavior

Swelling kinetics study

Samples of uniform dimension were cut from the sheet, gently wiped to remove dust, weighed and then poured in toluene at room temperature. After fixed tome interval, the sample was taken out, carefully wiped with a tissue paper to remove toluene adhered on the surface and finally weighed in a digital balance to determine amount of the toluene absorbed. Weight swelling was calculated using eq. (5).

$$Q_t = (W_f - W_i)/W_i \quad (5)$$

W_f denotes weight after solvent absorption and W_i is the initial weight of the sample. Q_∞ denotes overall swelling parameter and it was calculated using same equation (eq. 5) only taking W_f as the equilibrium swollen weight.

The weight swelling data were fitted to a power law equation (eq. 6) to calculate swelling kinetics.

$$W_f/W_i = kt^n \quad (6)$$

k and n are constants. Taking log on either side

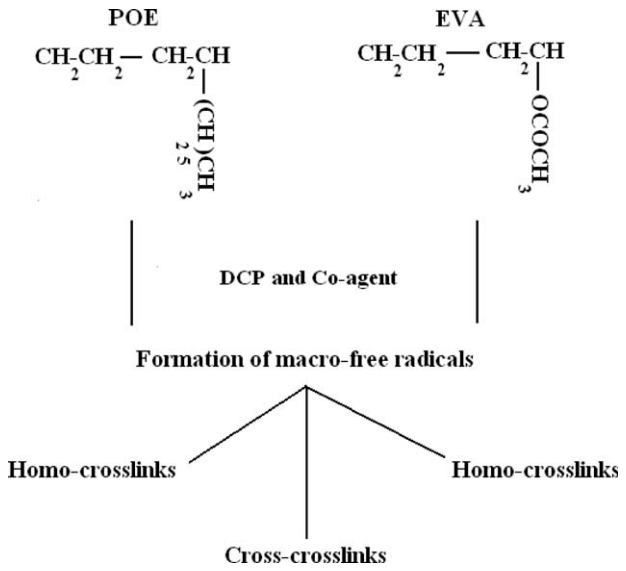

Scheme 1 Possible chemical crosslinks in reactive blending of POE and EVA

$$\ln(W_f/W_i) = \ln k + n \ln t \quad (7)$$

k depends on the penetrant (solvent) size and n governs solvent transport mechanism. n for all the network hybrids were calculated from the slope of the double logarithmic plot of the parameters in eq. (7).

Determination of sorption and diffusion coefficients

Solvent sorption coefficient, S, was calculated using eq. (8).

$$S = W_{s\infty}/W_i \quad (8)$$

$W_{s\infty}$ denotes equilibrium solvent weight.

Diffusion coefficient was calculated using eq. (9).

$$D = \pi(h\theta/4W_{s\infty})^2 \quad (9)$$

h is the sample thickness, θ denotes slope of initial portion of the plot of Q_t versus $\sqrt{t}$, and $W_{s\infty}$ is the equilibrium mole percent solvent uptake.

RESULTS AND DISCUSSION

Interpenetrating networking between polymers in melt is extremely difficult to achieve since sequential route cannot be adopted. We tried to optimize between self-crosslinking and efficient phase mixing of POE and EVA by separate intermixing of either POE or EVA with DCP and coagent at lower temperature (Stage I mixing) before final blending (Stage II mixing) assuming that it would result in sufficient number of homo-free radicals. Homo and cross reactions between these macroradicals in final stage are statistically equiprobable but physically it depends on several intrinsic factors. Fate of these macroradicals produced in Stage I mixing is schematically displayed in Scheme 1.

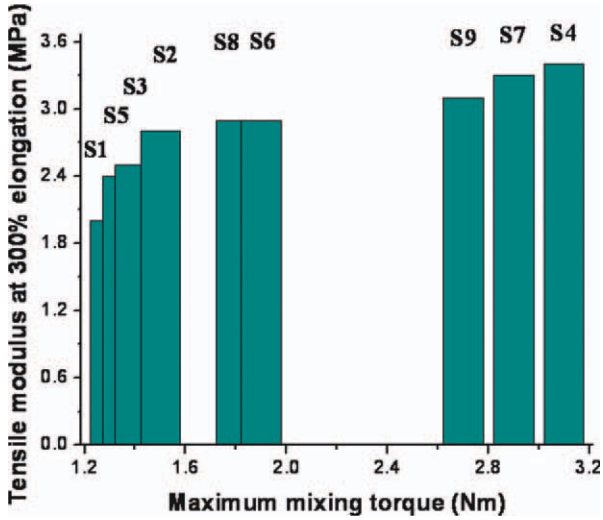

Figure 1 Correlative plot between 300% tensile modulus and maximum mixing torque of POE-EVA network blends achieved at Stage II mixing. [Color figure can be viewed in the online issue, which is available at wileyonlinelibrary.com.]

Figure 1 is a correlative plot between maximum mixing torque attained at Stage II mixing and the 300% tensile moduli of POE-EVA network blends. Mixing torque reflects melt viscosity of the blends which usually is proportional to their modulus. A sample mixing curve is shown in Figure 2 for blends with equal EVA content (12.6 wt %). Torque reaches its maxima within few seconds especially for S4 and S7 and then immediately declines and attains steady state with a value lower than the maxima. S1 in this figure has shown the slowest rise in torque. DCP

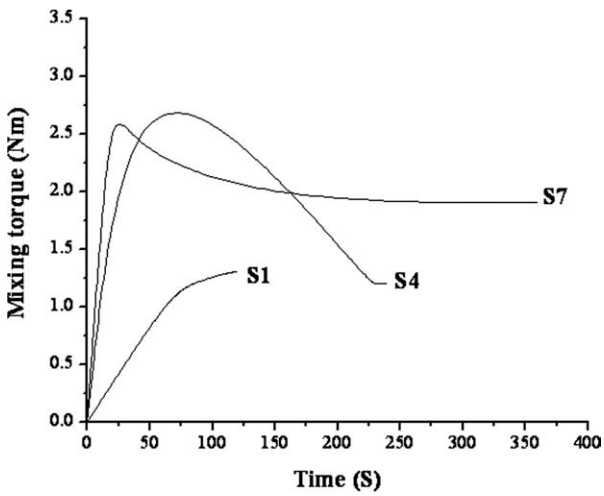

Figure 2 Representative time-torque profile of POE-EVA network blends of Stage II mixing—the blends are of equal POE:EVA weight proportions.

TABLE II
Mechanical Properties (Average), Infrared Spectroscopy, Gel Content, Contact Angle, and Solvent-Swelling Data on POE-EVA Network Blends

Properties	S1	S2	S3	S4	S5	S6	S7	S8	S9
Tensile strength[a] (MPa)	8.4	6.7	6.2	4.9	8.1	7.7	4.1	6.3	7.3
Tensile modulus (300%) (MPa)	2.0	2.8	2.5	3.4	2.4	2.9	3.3	2.9	3.1
Elongation at break[b] (%)	1559	1518	1502	673	874	368	487	362	334
Gel content[c] (%)	71.8	81.1	78.7	88.0	67.0	89.7	85.4	92.2	89.3
FTIR spectroscopic peak intensity ratio	0.84 (More EVA)	0.80 (More EVA)	0.78 (More EVA)	0.74 (More EVA)	0.56 (More EVA)	0.21 (More POE)	0.20 (More POE)	0.65 (More EVA)	0.22 (More POE)
Stress relaxation (S)	13.55	15.15	13.88	13.88	9.25	5.88	5.38	11.9	5.32
Contact angle[d]	45	37	33	53	47	41	54	55	57
Swelling index (Q_∞)	5.283	5.821	6.298	3.973	4.988	5.495	3.888	3.619	3.834
Sorption coefficient (S)	4.87	5.36	5.80	3.66	4.59	5.06	3.58	3.61	3.57
Diffusion coefficient ($D \times 10^7$ cm^2/S)	3.74	3.79	5.28	4.57	4.15	4.48	5.64	4.29	7.18

[a] Tensile strength of neat POE is 5.7 MPa and of neat EVA is 6.2 MPa.
[b] Elongation at break of neat POE is >600% and of neat EVA is >500%.
[c] Gel content of neat POE prepared with 1% DCP and 1% co-agent, blended at 180^0 C for 4 min amounts to 63% and in neat EVA, prepared using same experimental conditions, it amounts to 82%.
[d] Contact angle values for neat POE and neat EVA surfaces are 63 and 42, respectively.

content in S4 was 1 phr and in S7 it was 2 phr. Stage II mixing temperatures were 180 and 220°C as compared with only 0.5 phr DCP and 180°C final mixing temperature for S1. This difference is clearly visible from the figure. Torque was raised mainly due to additional crosslinking at the final stage. Extremely fast rise is attributed to faster reactions between already existent free radicals on the macrochains from stage I mixing. But torque-maxima are lowered due to "heat-softening" effect with time. Results displayed in Figure 1 have shown excellent parity between these two parameters and is in good agreement with the theoretical reasoning. Results on gel content and tensile properties of the blends are reported in Table II.

Separate statistical analysis was carried out to determine which, among the blending factors, had highest influence on these properties. A sample calculation for gel content analysis has been demonstrated for ready understanding. A total of 10 trials were carried out for each sample on gel content measurement. The SN (signal to noise) ratio for each experiment was computed for the target value case, a response chart was created and the parameters were determined that have highest and lowest effect on the gel content. Following eqs. (10–14) was used in steps to calculate SN ratio.

$$P_{m1} = (72.1 + 75.2 + 69.5 + 70.6 + 72.6 + 71.2 + 70.3 + 72.5 + 72.3 + 72.1)^2/10 = 51635.72 \quad (10)$$

$$P_{T1} = 72.1^2 + 75.2^2 + 69.5^2 + 70.6^2 + 72.6^2 + 71.2^2 + 70.3^2 + 72.5^2 + 72.3^2 + 72.1^2 = 51658.23 \quad (11)$$

$$P_{e1} = P_{T1} - P_{m1} = 51658.23 - 51635.72 = 22.51 \quad (12)$$

$$V_{e1} = P_{e1}/(N-1) = 22.51/9 = 2.50 \quad (13)$$

$$SN_1 = 10\log[(P_{m1} - V_{e1})/NV_{e1}] = 33.61 \quad (14)$$

Table III is the overall SN ratio table computed on gel content study for all nine blend samples. Table IV is the response table created based on SN ratio for each set of parameters. As for example, eqs. (15)–(17) demonstrates this in respect of EVA content in the blends.

$$SN_{B1} = (33.61 + 28.89 + 26.76 + 25.21 + 26.85 + 32.59 + 27.52 + 32.61 + 29.70)/9 = 29.30 \quad (15)$$

$$SN_{B2} = (24.71 + 31.08 + 31.38 + 30.62 + 29.01 + 24.62 + 25.37 + 26.35 + 29.02)/9 = 28.02 \quad (16)$$

$$SN_{B3} = (26.66 + 26.93 + 26.02 + 25.21 + 26.05 + 25.92 + 26.12 + 27.01 + 26.35)/9 = 26.25 \quad (17)$$

TABLE III
Signal to Noise Ratio of Each POE-EVA Blends on Gel Content Measurement

Samples	A (Peroxide)	B (EVA)	C (Temp)	D (Time)	SN
S1	1	1	1	1	33.61
S2	2	1	3	2	34.25
S3	3	1	2	3	26.60
S4	1	2	2	2	28.83
S5	2	2	1	3	31.02
S6	3	2	3	1	26.87
S7	1	3	3	3	29.57
S8	2	3	2	1	30.78
S9	3	3	1	2	27.25

TABLE IV
Response Table for Gel Content Analysis

Level	A (Peroxide)	B (EVA)	C (Temp)	D (Time)
1	25.95	29.30	24.66	25.06
2	23.37	28.02	23.38	24.14
3	23.03	26.25	23.73	22.57
Δ	2.92	3.05	1.28	2.49
Rank	2	1	4	3

The effect of this factor (EVA content) is then calculated by determining the range (eq. 18) and finally the rank is assigned.

$$\Delta = \text{Max} - \text{Min} = 29.30 - 26.25 = 3.05 \qquad (18)$$

Lowest rank assigned against any factor illustrates maximum influence of that particular factor on the property under study. In this case, it is EVA concentration in Table IV that has largest influence on the amount of gel formed while the final blending temperature has the least. However in statistical calculations, the general inference drawn cannot be true for all individual data since each result comes from combination of different sets of physical parameters. One such example is S5. It has 25.1 wt % EVA content but has produced lower gel than the sample with low EVA content (12.6 wt %). Interestingly, peroxide concentration is the second largest influencer on the gel content since increase in peroxide concentration generates more reactive sites on either POE or EVA. Reaction time and temperature has been found to be least significant in this case. This tend corroborates our previous study where increase in concentration of both modifier (ethylene-*co*-acrylic acid) and crosslinker (dicumyl peroxide) in POE had increased gel content of the blends as the modifier macromolecule with shorter side chain was the favorable place for radical formation.[15] "Chain scission" is incidental with crosslinking in reactive blending. Charlesby Pinnar calculation gives a reasonably good rational measure of that. Figure 3 shows this plot for network blends with variable EVA content since it is the prime influencer. Slope and intercept values from the linear fit of three discrete data sets in Figure 3 are calculated. Blends with 12.6 wt % EVA contents show lowest intercept but highest slope (intercept: 0.308; slope: 0.207). Samples with 25.1 wt % EVA show the reverse—it has lowest slope and highest intercept (intercept: 0.498; slope: 0.111). Further increase in EVA concentration to 50.0 wt % results intermediate slope and intercept values (intercept: 0.357; slope: 0.173). Higher slope in Charlesby Pinnar plot indicates low crosslinking whereas higher intercept elucidates higher chain scission (eq. 2). According to Figure 3, extent of crosslinking with 12.6 wt % EVA containing network blends are little lower while it is moderate to high in blends with 50.0 and 25.1 wt % EVA contents—best being the group of blends with 25.1 wt % EVA. The tendency towards chain scission, accordingly, has shown parallel trend since more crosslinking generally would also give more chain degradation effect. The order of chain degradation is: blends with 25.1 wt % EVA> 50.0 wt % EVA> 12.6 wt % EVA.

Evaluation of majorly crosslinked phase in IPN gels delineates its bulk phase morphology. It was studied using FTIR spectroscopic peak intensity ratios. FTIR spectroscopy is an effective tool for phase quantification if a calibration curve is known.[15,18] Peak intensity ratio of the absorbances at 1710 cm^{-1} of C=O in EVA and at 720 cm^{-1} of pendant $(CH_2)_5CH_3$ unit in POE was considered as the relative measure of predominance of either of these phases in the insoluble gels after comparing with a calibration plot (not shown here) of known blend composition. The results are reported in Table II with a clear mention of relative predominance of the particular phase in the extracted gel. One extreme of this data set should be 0 and that is for neat POE (absorbance at 1710 cm^{-1} is absent). This is an absolutely relative measure of the phases where higher peak intensity ratio indicates predominance of EVA while the reverse is true for POE in the blends. Figure 4 displays TEM images of selective network hybrids with different crosslinked phases. Images are taken in unstained state but phase distinction is clear due to density differences. EVA has lower MFI and is denser so appears darker than POE in these images. POE forms the continuous phase due to its high MFI. Crosslinked domains have withered and appear as distributed phase. S6 and S7 show

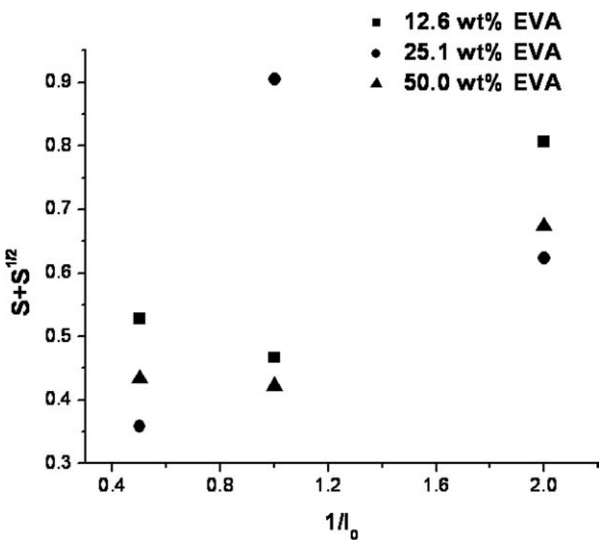

Figure 3 Charlesby Pinar plot of POE-EVA network blends.

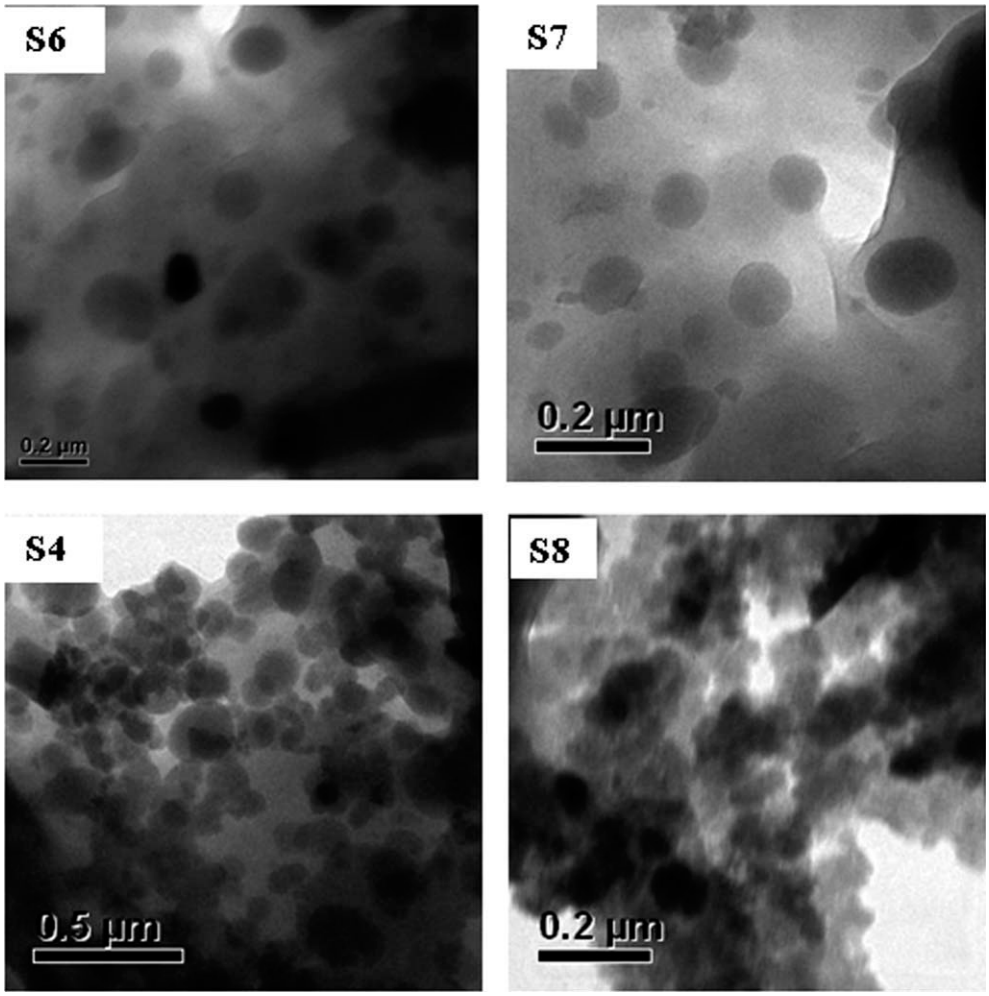

Figure 4 TEM photomicrographs of selective network hybrids.

predominantly crosslinked POE domains since these have close shade match with the continuous phase in these blends. It meticulously corroborates FTIR spectroscopic claims (Table II). Similarly, S4 and S8 show majorly crossslinked EVA domains. S8 has produced highest gel when extracted (Table II). It shows some shriveled POE domains along with EVA in the photomicrograph since both of these phases are crosslinked.

Tensile properties (averaged over ten samples) of different blends are reported in Table II. It is observed that some blends have shown synergism in some of the properties since these are convincingly higher than either of the neat elastomers, POE and EVA, mentioned as addendum to Table II. As for example, samples like S5, S6, and S9 have shown better tensile strengths but their tensile moduli and overall elongations are not concomitant. Another such example is S1. It has shown highest tensile strength and overall elongation but lowest modulus. Average gel content of this sample is also in the lower range. Interestingly, S1–S3 has produced very high elongation and S4 onwards, it has drastically reduced. Response analysis of this data set in Table V shows that peroxide concentration plays the key role in governing tensile strength and overall elongation properties while EVA concentration influences tensile modulus of the network blends. Tensile strength and elongation at failure—both are bulk properties and depend on morphological status, i.e., samples with higher modulus can often show low tensile strength and can fail early due to stress concentration around defects/flaws inside (S4 and S7). Increased peroxide concentration can often restrict

TABLE V
Response Analysis of Tensile Properties of POE-EVA Blends

Parameters	EVA	Peroxide	Temperature	Time
Tensile strength	2	1	3	4
Tensile modulus (@300%)	1	2	3	4
Ultimate elongation	2	1	3	4

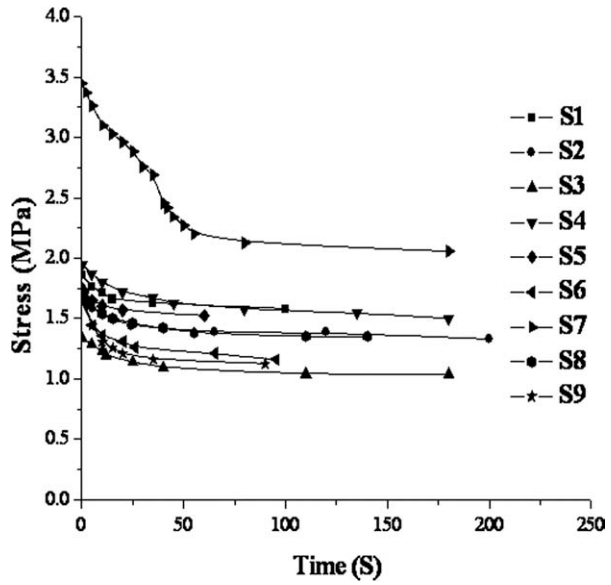

Figure 5 Stress relaxation plots of POE-EVA network blends.

phase mixing due to high crosslinking but at the same time proper combination of other factors like reaction temperature and time can overhaul and result into phase homogenization. In contrast, some of the samples like S4 and S7 show inferior tensile strength and overall elongation values than the neat samples due to improper combination of levels of different parameters. Tensile modulus, theoretically, depends on gel content of the blends since higher crosslinking often results in stiffer molecules. A parallel correlation has been found in this case. Gel content of the blends was maximally influenced by EVA concentration which in turn affects 300% modulus values. More stringent mechanical properties like stress relaxation and hysteresis properties which strongly depend on blend morphology are discussed in the subsequent sections for better understanding.

Relaxation is an intensive material property and is a measure of the extent by which it comes back to its original state on release of external disturbance (stress). Stress relaxation experiment was carried out to understand elastic-plastic transition behavior in these double network blends. Relaxation behavior of single elastomer systems has been extensively studied and reported[19–22] but studies on complex, double network blend such as these are truly rare. All the relaxation curves are displayed in Figure 5. Exact exponential nature of relaxation curves are obtained with all nine network blends which are rarely observed in either gum or filled elastomers. Except S7, relaxation curves for rest of the blends lie in close proximity whereas in S7, it lies far above these set of values. It may be recalled that S7 has recorded very high modulus but its tensile strength was quite low. The relaxation time λ in seconds for all the samples are calculated and are reported in Table II. Since all the blends are predominantly double networked, we first tried to correlate relaxation time of each blend with their gel content data for elucidation. In fact, there is no correlation found between gel content data and relaxation time. But one important observation is that the blends with higher gel content are relaxing faster than those with low gels and this is truly anomalous to theoretical understanding. As mentioned, double network system is a complicated case and so its performance analysis using conventional approach seems difficult. Thus "distribution of crosslinks" instead of "extent of crosslink" was considered as the next basis for explanation. Figure 6 gives the extract of this. Now it is clearly seen that blends with predominantly crosslinked POE has relaxed faster than when reverse has happened. It means relaxation is a function of mutual predominance of either of crosslinked POE or EVA phases rather than overall gel content in a double network blend. POE has slightly better flow behavior than EVA as its MFI is little higher. Higher segmental mobility is therefore still expected even after POE molecules get crosslinked. Conversely, EVA chains are little stiffer (higher T_g than POE) due to presence of pendant vinyl acetate groups and these segments further stiffens up on crosslinking. High segmental mobility causes faster relaxation while reverse is true for stiffer chain segments.[23] Synonymous explanation can therefore be cited for critical understanding of elongation at break data reported in preceding section. Samples with freer

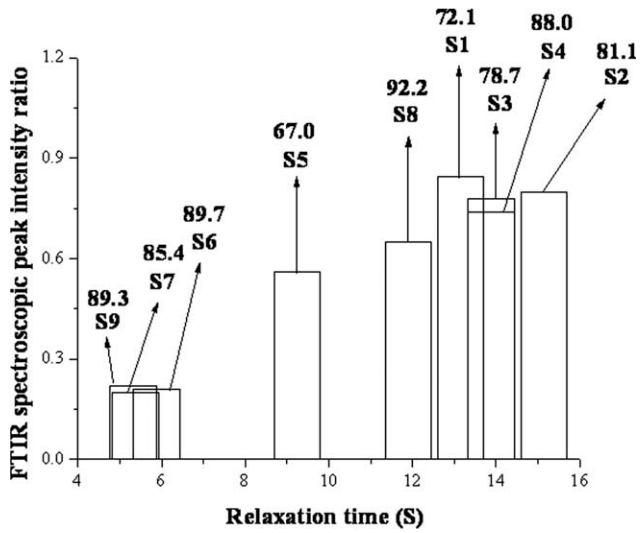

Figure 6 Correlative plots of FTIR peak intensity ratio, stress relaxation time, and gel content of POE-EVA network blends.

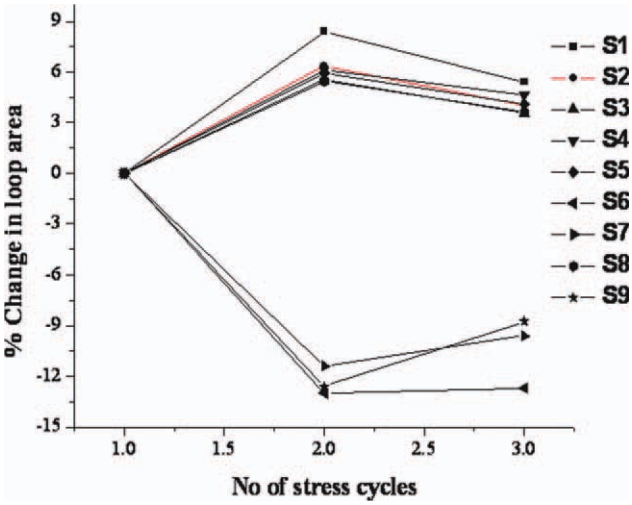

Figure 7 Percent change in hysteresis loop area against number of stress cycles in POE-EVA blends; negative value indicates drop in area than the previous one while positive value indicates the reverse. [Color figure can be viewed in the online issue, which is available at wileyonlinelibrary.com.]

POE phase (S1–S5 but not S8) have elongated more than those with more uncrosslinked EVA portions.

For all viscoelastic (solid) materials, a measurable part of the work expended in deforming the solid is dissipated as heat. It is a common experience that the load-elongation curve followed during loading or extension is not the same as that conformed during unloading or retraction. The work of stretching during loading is measured by the area under the curve of extension or loading. Similarly, the area under the unloading curve gives a measure of the work of retraction. The area encompassed between the loading and unloading curves, called the hysteresis loop, gives a measure of the mechanical energy dissipated as heat. The hysteresis loss for an ideally elastic (Hookian) body is zero as the loading and unloading curves are one and the same and there is no loop. For non-Hookian, i.e., imperfectly elastic or viscoelastic bodies, the hysteresis loop is measurable and the area of the loop is dependent on the degree of structural changes brought about during extension due to uncoiling or unfolding of the molecular chains.

Hysteresis in a crosslinked sample measures extent of reform able chemical bonds exists under cyclic mechanical stress. The energy difference between loading and unloading stress cycles is called viscous loss. In cyclic loading another important factor is Mullins effect, which in crosslinked rubbers, as a general case, does not truly disappear even after several cycles. In present set of nine samples, each has been taken for three consecutive loading–unloading cycles with no time allowed for equilibration in between. The area inside loading–unloading cycle has been calculated and the results are shown as percent change in area from the first cycle (positive for increase and negative for decrease) in Figure 7. Results show an interesting trend. "All" double network blends did not exhibit stress-softening behavior (Mullins effect) particularly those where EVA has formed major crosslinked phase. Examples of such samples are S1, S2, S3, S4, S5, and S8. Blends with POE as major crosslinked phase displayed stress-softening effect after multiple stress cycles. Such blends are S6, S7, and S9. A recent experiment of Webber et al.[24] with double network swollen hydrogels shows stress softening effect once the reverse cycle was delayed. We experimented with no time lag in between subsequent cycles and so it is more critical in our case for the blends to exhibit reformation characteristics of the already broken bonds in forward stress path for stress softening. Gradual lowering of plot area (hysteresis loop) in samples like S6, S7, and S9 indicates existence of such chemical bonds that can be reformed quickly on withdrawal of the applied stress. All of these samples have shown faster stress dissipation as well. Rest of the samples show high to higher viscous loss on application of multiple stress cycles mainly due to stiffer EVA dominant crosslinks that is not easy to reform after stress withdrawal. Accordingly these samples have shown slower relaxation and low elongation behaviors.

Extensive swelling studies greatly manifest architecture of the network hybrids described so far. In addition, it provides excellent scientific support towards physico-mechanicals explained in preceding sections. Figure 8 shows the kinetic investigation on

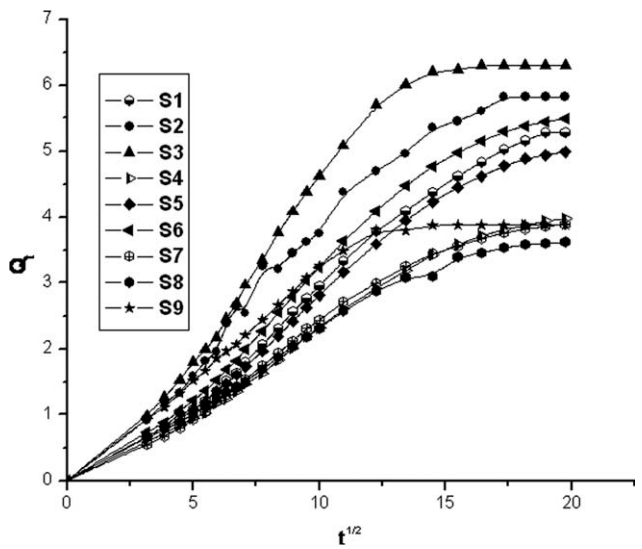

Figure 8 Solvent-swelling kinetics of the network hybrids studied in toluene at room temperature.

swelling action of the network hybrids in toluene. It was observed that EVA has greater affinity towards toluene than POE. But results described in Figure 8 clearly shows that the rate and extent of swelling (swelling index, Q_∞) are equally influenced by other factors like distribution (and nature) of crosslinks and overall gel content apart from EVA concentration in the blends. As for example, S5 has the minimum gel and moderately higher EVA content but still it swells much slower than samples like S2, S6 having much higher gel fraction. Similarly S6 and S9, in spite of having higher gel contents, swell quite fast due to mutual effects of high EVA content (50.0 wt %) and presence of more flexibly crosslinked POE phase in its structure. S7 does have more crosslinked POE fraction but due to least EVA content, it swells quite slowly. Finally, net decreasing order of swelling rate appears as S3 > S2 > S6 (and S9, up to certain time interval)> S1 > S5 > S9 > S4 ≈S7 > S8 (Fig. 8). Overall solvent uptake values (Q_∞) show almost similar trend (Table II). The results are in strict concurrence with intrinsic mechanical properties like stress relaxation and hysteresis experiments described earlier. The solvent transport mechanism was truly Fickian since the index n in the kinetic expression (eq. 7) is < 0.5 for all the blends. The k values are not considered since it expresses chemical nature of the diffusing molecules which is identical (toluene) in all cases.

The transport phenomenon of solvent molecules through the hybrids generally abides by-sorption, diffusion, and desorption mechanisms. Desorption is least significant among these three in understanding network architecture. Sorption mechanism is surface controlled and should be governed by the EVA concentration at the surface. Higher EVA content would attract more toluene since it has greater affinity. Sorption data can, therefore, be complemented by contact angle data. Hydrophobic–hydrophilic property of any solid surface can be well described by the interfacial angle of contact between surface liquid drop say of water and that solid surface. Lower the contact angle value, more polar the surface is. Table II shows these values for all the nine network hybrid samples. Although there is no strict correlation between EVA content and surface polarity in these reactive blends but contact angle values tallies well with the respective sorption coefficients (S, calculated using eq. 8). Diffusion coefficients usually mimic relaxation behavior since transport phenomenon is controlled by Ficks law where the distribution and nature of crosslinks but not the sorption behavior is more likely to affect diffusing solvent molecules. Diffusion coefficients were calculated using eq. (9) and the results are reported in Table II. Samples like S6, S7, and S9 have shown faster diffusion of toluene in spite of fairly high gel content. Conversely, it is relatively slow in rest of the network hybrids among which some have markedly lower gel contents; as for example, S1 and S5. Earlier it was established that more flexible POE forms dominant crosslinked phase in the samples, S6, S7, and S9, whereas crosslinked EVA dominates in rest of the samples. Understandably, smaller molecules like toluene would prefer flexible network to diffuse in since it is less resistive as in S6, S7, and S9, whereas would move at a slower pace in rest of the hybrids having slightly more rigid networks.

CONCLUSION

In conclusion, design parameters of S5 are approved as the best since it exhibits maximum balance between preferred physico-mechanicals and solvent resistance properties. The column reporting different properties of S5 in Table II and its design variables in Table I are marked with a shade for distinction. Taguchi technique has, therefore, provided an excellent way of optimizing material properties using fewer experiments based on selected design parameters and levels. S5 has the net polarity gain of 10% and it has modified POE in the most balanced way within the periphery of selected design variables. This idea could now be extended for designing several other industrial products in future.

References

1. Liu, J.; Yu, E. C.; Zhou, C. Polymer 2006, 47, 7051.
2. Steve Chum, P.; Swogger, K. W. Prog Polym Sci 2008, 33, 797.
3. Dangtungee, R.; Desai, S. S.; Tantayanon, S.; Supaphol, P. Polym Test 2006, 25, 888.
4. Svoboda, P.; Theravalappil, R.; Svobodova, D.; Mokrejs, P.; Kolomaznik, K.; Mori, K.; Ougizawa, T.; Inoue, T. Polym Test 2010, 29, 742.
5. Svoboda, P.; Svobodova, D.; Slobodian, P.; Ougizawa, T.; Inoue, T. Euro Polym J 2009, 45, 1485.
6. Svoboda, P.; Svobodova, D.; Slobodian, P.; Ougizawa, T.; Inoue, T. Polym Test 2009, 28, 215.
7. Biswas, A.; Bandyopadhyay, A.; Singha, N. K.; Bhowmick, A. K. J Appl Polym Sci 2009, 114, 3906.
8. Biswas, A.; Bandyopadhyay, A.; Singha, N. K.; Bhowmick, A. K. J Mater Sci 2009, 44, 3125.
9. C. Jiao, Z.; Wang, Z.; Gui, Y. H. Euro Polym J 2005, 41, 1204.
10. Ray, S.; Bhowmick, A. K. Rad Phys Chem 2002, 65, 259.
11. Korobko, A. P.; Bessonova, N. P.; Krasheninnikov, S. V.; Konyukhova, E. V.; Drozd, S. N.; Chvalun, S. N. Diamond Relat Mater 2007, 16, 2141.
12. Jha, A.; Bhowmick, A. K. Polym Degrad Stab 1998, 62, 575.
13. Laurienzo, P.; Malinconico, M.; Martuscelli, E.; Volpe, M. G. Polymer 1989, 30, 835.
14. Al-Malaika, S.; Kong, W. Polymer 2005, 46, 209.

15. Gupta, B.; Banerjee, D.; Goswami, L.; Bandyopadhyay.A. J. Appl Polym Sci 2011, 120, 3401.
16. Tai, H-J. Polymer 2001, 42, 5207.
17. Ross.P. J., Eds. Taguchi Techniques for Quality Engineering: Loss Function, Orthogonal Experiments and Tolerance Design, McGraw Hill Book Company: USA, 1998; Chapter 3.
18. Lee, J.; Lee, K. J.; Jang, J. Polym Test 2008, 27, 360.
19. Baeurle, S. A.; Hotta, A.; Gusev, A. Polymer 2005, 46, 4344.
20. Ronan, S.; Alshuth, T.; Jerrams, S.; Murphy, N. Mater Des 2007, 28, 1513.
21. Cantournet, S.; Desmorat, R.; Besson, J. Inter J Solids Struct 2009, 46(11–12), 2255.
22. Bartenev, G. M.; Kucherskii, A. M.; Radayeva, G. I. Polym Sci U.S.S.R. 1981, 23, 313.
23. Tager, A, Eds. Physical Chemistry of Polymers, 2nd ed.; Mir Publishers: USSR, Moscow, 1978; Chapter 4.
24. Webber, W. E.; Creton, C.; Brown, H. R.; Gong, J. P. Macromolecules 2007, 40, 2919.